Proceedings of the 28th IEEE
EMBS Annual International Conference
New York City, USA, Aug 30-Sept 3, 2006

Central Physiological Tremor Oscillators within a Hemifield Repetitive Visual Stimulation Paradigm

Monica-Claudia Serban, *Student Member, IEEE,* Dan Marius Dobrea, *Associate Member, IEEE*

***Abstract*—In order to analyze the activation pattern of the two putative central tremor oscillators that independently control the right and left hands, two hemifield repetitive visual stimulation tests were employed. The dynamical evolution of the tremor spectral characteristics of both hands was tracked using coherence joint time-frequency analysis. To get reliable spectral estimators for the tremor stochastic process, two non-parametric methods were applied: a Welch periodogram-based method and a multitaper method. In both cases, the results were the same: none significant coherence value could indicate a potential central driving activity.**

I. Introduction

Physiological hand tremor (PT) has been often considered a source of unwanted noise in the motor system. In this view, either the PT [1] or its pathological manifestations [2] were treated as motor outputs that should be damped out or controlled. Unlike this approach, another, more recently, point of view regarding the tremor is that its inspection can provide physicians with a more accessible way to understand the organization and activity of the human neuromotor system. Now, it is largely admitted that the PT has a multifactorial origin, with contributions not only from motor unit firing properties, mechanical resonances and reflex loop resonances, but also, from the central nervous system (CNS). Accordingly, the analysis of tremor is suggested to be particularly suited for studying the central corresponding oscillations (especially in human investigations, where the direct central recording has its obvious limitations). Moreover, several possible functional roles ascribed to the tremor are reviewed in [3]. All these roles are related to the neurogenic components of the tremor and, especially, to the fact that a cortical (central) – motor (peripheral) common rhythmicity was confirmed by the presence of a synchronized discharge of corticomotor neurons at certain preferred frequencies [4][5][6][7][8][9][10][11].

The different peripheral synchronization patterns encountered in the limb – and related to the neurogenic components of the tremor – are likely to be the result of some similar mechanisms also invoked in the respiratory system, namely: a) synchronization due to the branched descending inputs (*short-term synchronization*), b) synchronization due to a common driving oscillator that also drives the descending inputs (*external* or *tuned synchronization*) and c) synchronization due to shared polysynaptic inputs, with each synapse introducing a temporal "jitter" in signal transmission (*long-term*, *pre-synaptic* or *broad-peak synchronization*) [3]. Among these three synchronization mechanisms only that of tuned synchronization allows the investigator for an external non-invasive possible control in the tremor analysis methodology. Specifically, a brain rhythm (steady-state visual/auditory evoked potentials, SSVEPs/SSAEPs) can be extrinsically driven (e.g. through visual/auditory repetitive stimulation); then, the presence of temporal (phase) relationship introduced between central induced oscillations and the peripheral tremor can be further investigated. Following these lines, the authors from [12] used the photic driving as a method of cortical activation and, then, they investigated the relationship between well defined SSVEPs and the simultaneously recorded PT signal. They found no such a relationship and, finally, concluded that even when a large and extremely periodic oscillation of some central neurons is induced by photic driving, its contributing to the tremor is so attenuated that it is practically undetectable by the methods they applied. In the end, they recommend the cross-correlation and coherence functions to be used in order to discover any possible hidden peak in the tremor, corresponding to the frequency of photic driving.

We used as well the photic driving paradigm in two previous communicated papers [13],[14]. In the last one the phase synchrony parameter was used in order to explain the significant coherence achieved [13] at double the stimuli frequencies for the PT. Since coherence mixes the amplitude information with that of phase, we investigated which of them – the amplitude or the phase synchronization – was responsible for this behavior. The recurrence plot of the phase shift and the statistical phase synchrony parameter were used to qualitatively and, respective, quantitatively estimate the phase synchrony. The two analyses conducted to the same result. None of them could confirm the importance of phase synchrony in the synchronization revealed by coherence as a function of the frequency *f*. Thus, we concluded that the other parameter, namely the amplitude, may play the major role in the coherence significant values. This can be explained by similar behavior (increasing or decreasing in the number of neurons recruited) concurrently manifested in both, the central

This work was supported by the Romanian National Council for Research in High Education, Grant Td 27637/14.03.2005, code 145

M.-C. Serban, D.M. Dobrea are with the Department of Applied Electronics and Intelligent Systems, "Gh. Asachi" Technical University, Iasi, Romania (serbanm@etc.tuiasi.ro, mdobrea@etc.tuiasi.ro).

oscillator and the oscillator governing the tremor generation process.

The PT signals analyzed in [13],[14] were acquired with the system proposed in [15]. In this paper, in order to get comparable results with those reported in the literature, we developed and used a new accelerometer based tremor acquisition system. Moreover, besides the aim of revisit the coherence function evaluation (as a method to explore how much the tremor signal is reflecting the synchronized cortical activity), two other objectives were proposed: a) to analyze the activation pattern of the two putative central oscillators proposed in [16] as independently controlling the right and left hands, and b) to search for some preferred coupling direction between these oscillators (as possible corresponding to the dominant hand).

II. Materials and Methods

A. Tremor acquisition

The tremor acquisition system was implemented with two low-g accelerometer sensors (ADXL203, Analog Devices), a National Instruments data acquisition board (AT-MIO-16E-10) and a software program that acquired simultaneously, and in synchronism with the visual stimuli, the tremor signal of both hands. On a single chip, the ADXL203 circuit embeds a high precision, low power, dual axis iMEMS (integrated Micro Electro Mechanical System) accelerometer, that measures acceleration with a full-scale range of ±1.7 g and a sensitivity of 1000 mV/g. The AT-MIO-16E-10 DAQ board was configured in the differential mode and acquired the tremor movement on 12 bits, with a sampling rate of 240 Hz. The low-pass filtering for antialiasing and noise reduction was implemented using the ADXL capability. An external capacitor was connected at each ADXL203 accelerometer. In this mode the signal 3 dB bandwidth was set at 151 Hz. The mass of the each accelerometer plus mounting plate was less than 5 g and the entire montage was positioned between the forefinger and the middle finger of the subject.

Two healthy right-handed adults (one man and one female), with normal or corrected-to-normal vision, served as volunteer subjects after giving informed consent. Their mean age was 30.1 (range 29 to 32) years. Additionally, they have been taken no kind of medication in the week previous to the recordings. All the recordings took place in a quiet room without any other source of light than that of the stimuli generator. The subjects were seated in front of a 17"-computer screen, the head stabilized with a chin rest at a constant viewing distance of 80 cm. Viewing was binocular and, during testing, the subjects had to maintain fixation on a central white cross while thinking at nothing and avoiding blinks or eye movements. They were instructed to use minimal effort to maintain their stretched hands in an approximately same horizontal position while having no visual control of them. For each subject and for each paradigm 40 trials were recorded, every trial taking 64 s. The elbows of the subjects were fixed and brief rests were allowed between each trial in order to avoid the arm fatigue influence.

In this study two different conditions were tested. In the *first paradigm* two stimuli were presented against a dark background at two different locations (left visual hemifield, LVH, and right visual hemifield, RVH). The stimuli were lined up along the horizontal meridian of a computer monitor set to a resolution of 1028 x 1024 pixels, with a refresh rate of 85 Hertz. Each stimulus was a white circle changing its luminosity between a black background and a white flash. Also, the stimuli subtended a viewing angle of 2.48 x 2.48 degrees, with an eccentricity of 10°12″ representing the distance between the inner edges of the circles to the central fixation cross. The stimulus in each visual hemifield was flickered at a different frequency (with a 50/50 on/off cycle): the stimuli from the LVH was flickered at rate of 7 Hz and only in the first 32 seconds, while the stimuli from the RVH was flickered at rate of 19 Hz and only in the last 32 seconds of a 64-seconds trial. Simultaneously with the stimuli the tremor signal from the both hands was recorded. In the *second paradigm* the stimuli presented above were simultaneously delivered to the subject during all 64 seconds of a trial. Another difference is that after the first 32 seconds of the experiment the stimuli exchanged their frequency characteristics (now, left stimulus – 19 Hz, right stimulus – 7 Hz) and remained so until the end of the recording.

B. Coherence Joint Time-Frequency Analysis

The aim of this study was to relate characteristics of the frequency content of left and right hand PT (experienced during concurrently or alternately hemifield visual repetitive stimulation) to the steady-state visual evoked potentials (SSVEP) induced at the visual level of corresponding cortical hemisphere. An available method to examine details of the time course of the frequency content that is widely used to study non-stationary time series (the case of tremor signal) is the *joint time-frequency analysis* (JTFA) [17] which expands signal in both time and frequency domain. Within this analysis the coherence function was used as a tool of studying the degree of linear correlation in the frequency domain between two signals on a scale from zero (independence) to one (complete linear dependence). Because the tremor signal is usually treated as a realization of a stochastic linear process [18], in order to design an accurate coherence time-frequency (TF) distribution estimator for tremor we had to consider also the bias/variance dilemma. For this reason, two nonparametric methods to compute coherence estimator were proposed: *periodogram* (*Welch*) *method* and, respectively, *multitaper method*. In JTFA, the coherence function estimator, $\gamma^2_{xy}(f,t)$, was calculated on a sliding window of constant length, L, with a sliding step, s. In order to increase the accuracy of the

spectral parameters, we averaged the spectral samples obtained in the corresponding time intervals for each N trials set acquired per task and per subject.

1) Welch method: This method was used to compute estimators for the auto and cross-power spectral density functions (applied in coherence formula), and it consisted in: **a**) partitioning the signal $x[n]$ ($n = 0 \div N_s\text{-}1$) into N_w sliding equal length segments (sliding step = n_w samples) by applying a window function, $w[n]$, of length, l (1):

$$y_i[n] = x_i[n] \bullet w[n] \quad (1)$$

with i representing the ith segment, $n \in [(i\text{-}1)\cdot n_w,\ (i\text{-}1)\cdot n_w + l]$. **b**) computing a periodogram of each segment (2), and then averaging the individual periodograms (3):

$$\hat{S}^{i}{}_{xx}(f) = \frac{1}{l}\left|\sum_{n=(i-1)\cdot n_W}^{(i-1)\cdot n_W + l} y_i[n] e^{-j2\pi fn}\right|^2 \quad (2)$$

$$\hat{S}_{xx}(f) = \frac{1}{N_w}\sum_{i=0}^{N_w-1} \hat{S}^{i}_{xx}(f). \quad (3)$$

By averaging an increasing number of windows, the variance of estimator is further reducing, but shorter segments are resulting in each window; this fact introduces a distortion in the estimate due to increased spectral leakage. This problem is addressed by using an appropriate window function that is, in fact, a tradeoff between resolution and leakage.

2) Discrete prolate spheroidal sequences (DPSS)*:* Unlike the Welch method that uses a a single taper (or "window"), with some irretrievable loss of information at the beginning and the end of the series, the multitaper method (MT), is a periodogram averaging scheme that uses *some orthogonal tapers* to obtain approximately *independent estimates* of the power spectrum *for the entire signal* and then combines them to yield an final estimate. In this mode, some of the lost information previously mentioned is recovered. The optimal windows used with MT method are the *Slepian sequences* or *discrete prolate spheroidal sequences* and they are the eigenvectors of the Toeplitz eigenvalue equation [19]:

$$\sum_{m=0}^{N-1} \frac{\sin 2\pi W(n-m)}{\pi(n-m)} v_m^{(k)}(N,W) = \lambda_k(N,W) v_n^{(k)}(N,W) \quad (4)$$

where: $n,k = 0 \div N\text{-}1$, N is the length of the eigenvectors (and of the signal, N_s), and W is a half-bandwidth that defines a small local frequency band centered around frequency f. From their construction (4), it results two important properties of the Slepian sequences: a) they are *orthogonal time-limited functions* (this allows for minimizing the spectral estimator *variance*) and b) their energy are *most concentrated in the frequency band* [$-W$, W], being given by the corresponding λ_k eigenvalue (important to minimize the estimator *bias*). As in the Welch method, in the MT method there is a data set-dependent "resolution" parameter, namely the time-bandwidth product, NW, which allows an optimal trade-off between bias and variance. Usually, the first $K = 2NW$ tapers with the largest eigenvalues ($\lambda_k \cong 1$) are used to form the estimate. Thus, as NW increases, the variance of the estimate decreases; however, spectral leakage increases too, due to the fact that the bandwidth of each taper is also proportional to NW. Anyway, compared to the Welch method, it was shown that the estimate of the MT method allows for an easier quantification of the bias and variance tradeoff. For a given $x[n]$ signal, $n = 1 \div N_s$, and a given frequency resolution, NW, this last estimate is obtained by averaging the K eigenspectra (5):

$$\hat{S}_{xx}(f) = \frac{1}{K}\sum_{k=0}^{K-1} \frac{1}{\lambda_k} |X_k(f)|^2 \quad (5)$$

where: $X_k(f)$ is called the kth eigencoefficient and $|X_k(f)|^2$ is the kth eigenspectrum. $X_k(f)$ is computed by applying $v^{(k)}$ to the entire length-N_s signal, $x[n]$, and, then, by taking the discrete Fourier transform:

$$X_k(f) = \sum_{n=0}^{N_S-1} x[n] v_n^k e^{-j2\pi fn} \quad (6)$$

3) Coherence function: The magnitude-squared coherence (MSC) estimate between two jointly stationary stochastic processes, $x[n]$ and $y[n]$, $n = 0 \div N_s\text{-}1$, is defined for N *realizations* of the two processes (*Welch method*) as [20]:

$$\hat{\gamma}^2{}_{xy}(f) = \frac{\left|\sum_{l=0}^{N-1} \hat{S}^{l}_{xy}(f)\right|^2}{\left[\sum_{l=0}^{N-1} \hat{S}^{l}_{xx}(f)\right] \bullet \left[\sum_{l=0}^{N-1} \hat{S}^{l}_{yy}(f)\right]} \quad (7)$$

where: $\hat{S}_{xy}{}^{l}(f)$ is the cross-spectral density estimator; $\hat{S}_{yy}{}^{l}(f)$ and $\hat{S}_{yy}{}^{l}(f)$ are the autospectral densities estimates for the lth realization of each of the two processes. For the case of the *multitaper method*, the same MSC estimate is given by:

$$\hat{\gamma}^2{}_{xy}(f) = \frac{\left|\sum_{l=0}^{N-1}\sum_{k=0}^{K-1} \frac{1}{\lambda_k} X^{l}{}_{k}(f) Y^{l}{}_{k}{}^{*}(f)\right|^2}{\left[\sum_{l=0}^{N-1}\sum_{k=0}^{K-1} \frac{1}{\lambda_k}\left|X^{l}_{k}(f)\right|^2\right] \bullet \left[\sum_{l=0}^{N-1}\sum_{k=0}^{K-1} \frac{1}{\lambda_k}\left|Y^{l}_{k}(f)\right|^2\right]} \quad (8)$$

where: X^{l}_{k}(f) and Y^{l}_{k}(f) are the eigencoefficients calculated for the lth realization of each of the two processes, $K \le 2NW$ is the number of tapers used and the asterisk denotes complex conjugation.

III. Results

First, the signals were filtered with a FIR 45 Hz low-pass filter and de-trended, using a polynomial 2nd order for removing slow drifts introduced by the tremor acquisition systems. The coherence JTFA was done for pairs of tremor signals as follows: left – right (LR) hands, left – left (LL), and, right – right (RR). The results depicted in fig. 1 are obtained for subject 1 and for N=40 trials/paradigm. The length of the JTFA sliding window was L=1024 samples (frequency resolution, df = 0.23 Hz for MT method) and the sliding step was s =12 samples (time resolution, dt=50 ms). The length of the Hanning window used in Welch method was l=256 samples (df =0.93 Hz), with a sliding step of 12 samples (N_w=64 windows). For the MT method a 3.5 time-bandwidth parameter (NW) was applied.

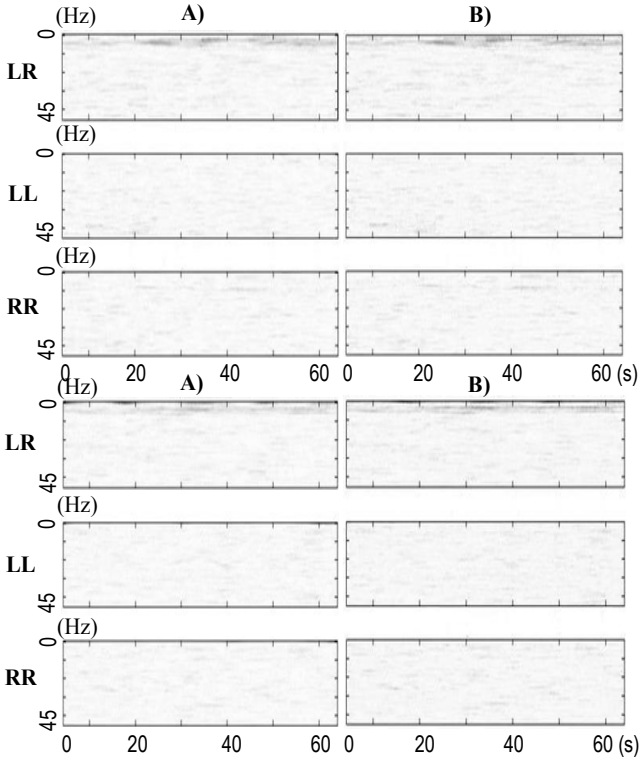

Fig 1. Coherence JTFA computed with: A), C) Welch method and B), D) Multitaper method. In A), B) is represented the 1st paradigm, and in C), D) the 2nd paradigm.

IV. Discussion and Conclusions

As we see from fig. 1, the differences between the coherence estimates computed with the two spectral methods are insignificant. Regarding the lack of any significant coherence value, this could: 1) confirm the hypothesis [12] that the hand PT is not influenced by repetitive photic brain stimulation, or 2) the SSVEPs were not obtained as expected, at the contralateral visual cortical level; this means that no central oscillators existed that could drive the hand tremor rhythms. It is known that the amplitude and phase of the SSVEPs are highly sensitive to stimulus parameters such as repetition rate, contrast or modulation depth, spatial frequency etc. Also, SSVEP amplitude is known to be larger for attended items than for unattended ones (our case). In this case, for a compelling analysis, a cortical activity monitoring (like EEG) is necessary in order to confirm and to allow the study of the central oscillators' activity as well.

References

[1] C. N. Riviere, S. R. Rader and N. V. Thakor, "Adaptive canceling of physiological tremor for improved precision in microsurgery", *IEEE Trans Biomed Eng*, vol. 45, no. 7, 1998, pp. 839–846

[2] M. Manto *et* al., "Dynamically Responsive Intervention for Tremor Suppression", *IEEE Eng Med Biol Mag*, May/June 2003, pp. 120 - 132

[3] J. H. McAuley and C. D.Marsden, "Physiological and Pathological tremors and rhythmic central motor control", *Brain*, Vol. 123, 2000, pp. 1545 – 1567

[4] S. Ohara *et* al., "Electrocorticogram-Electromyogram Coherence During Isometric Contraction on Hand Muscle in Human", *Clin Neurophysiol*, Vol. 111, 2000, pp. 2014 - 2024

[5] J. Raethjen et *al.*, "Is the Rhythm of Physiological Tremor Involved in Cortico-Cortical Interactions?", *Mov Disord*, Vol. 19 (4), 2003, pp. 458 - 465

[6] S. F. Farmer, "Rhythmicity, Synchronization and Binding in Human and Primate Motor Systems, [Review]", *J Physiol*, Vol. 509, 1998, pp. 3 - 14

[7] V. N. Murthy *et al.*, "Synchronization of Neurons During Local Field Potential Oscillations in Sensorimotor Cortex of Awake Monkeys", *J. Neurophysiol*, Vol. 76, 1996, pp. 3968-3982

[8] J. H. McAuley *et al.*, "Common 3- and 10-Hz Oscillations Modulate Human Eye and Finger Movements While They Simultaneously Track a Visual Target", *J Physiol*, Vol. 515 (3), 1999, pp. 905 - 917

[9] J. H. McAuley *et al.*, "Human Anticipatory Eye Movements May Reflect Rhythmic Central Nervous Activity", *Neuroscience*, Vol. 94 (2), 1999, pp. 339 - 350

[10] J. H. McAuley *et al.*: "Frequency Peaks of Tremor, Muscle Vibration and Electromyographic Activity at 10 Hz, 20 Hz and 40 Hz During Human Finger Muscle Contraction May Reflect Rhythmicities of Central Neural Firing", *Exp Brain Res*, Vol. 114 (3), 1997, pp. 525 – 541

[11] D. E. Vaillancourt and K. M. Newell, "Amplitude Changes in the 8-12, 20-25, and 40 Hz Oscillations in Finger", *Clin Neurophysiol*, vol. 111 (10), 2000, pp. 1792 – 1801

[12] M. Lakie and N. Combes, "The Phase of Postural Hand Tremor is not Influenced by Repetitive Photic Brain Stimulation", *Clin Neurophysiol*, Vol. 110, 1999, pp. 2020 - 2025

[13] M. C. Serban, D. M. Dobrea and H. N. Teodorescu, "Evidence for the Central Oscillators in the Physiological Tremor Generation Process", CD-Proceedings of the 4th European Symp. In *Biomed Eng*, Session 4, Patras, Greece, June 25th - 27th, 2004

[14] M. C. Serban and D. M. Dobrea, "A Phase Analysis of the Hand Tremor Signal in a Photic Driving Paradigm", Proceedings of the 14th Int Conf of Med Phys, pp. 1547-1548, ISSN 0939-4990, Nuremberg, Germany, September 14th - 17th, 2005

[15] D. M. Dobrea, H. N. Teodorescu, and D. Mlynek, "An interface for virtual reality applications", *Rom. J. of Inform Sci Tech*, vol. 5, no. 3, 2002, pp. 269–282

[16] B. Koster *et al.*, "Central mechanisms in human enhanced physiological tremor", *Neurosci Lett*., vol. 241 (2-3) , Jan 30 1998, pp. 135-138

[17] R. Vio, W. Wamsteker, "Joint Time–Frequency Analysis: a tool for exploratory analysis and filtering of non-stationary time series", *http://arxiv.org/abs/astro-ph/0204186*, 10 April 2002, pp. 1–15

[18] J. Timmer, "Modeling noisy time series: physiological tremor", *Int J Bifurcat Chaos Appl Sci Eng*, vol. 8, no. 7, 1998, pp. 1505-1516

[19] D. Slepian, "Prolate spheroidal wave functions, Fourier analysis, and uncertainty – V: the discrete case", *Bell Syst. Tech. J.*, vol. 57, 1978, pp. 1371-1430

[20] S. Wang, and M. Tang, "Exact confidence interval for magnitude-squared coherence estimates", *IEEE Signal Process Lett*, vol. 11, no. 3, March 2004, pp. 326-329